STEM CELLS®

STEM CELL TECHNOLOGY: EPIGENETICS, GENOMICS, PROTEOMICS AND METABONOMICS

Comprehensive Proteomic Analysis of Mesenchymal Stem Cell Exosomes Reveals Modulation of Angiogenesis via NFkB Signaling

JOHNATHON D. ANDERSON[1], HENRIK J. JOHANSSON[2], CALVIN S. GRAHAM[1], MATTIAS VESTERLUND[2], MISSY T. PHAM[1], CHARLES S. BRAMLETT[1], ELIZABETH N. MONTGOMERY[1], MATT S. MELLEMA[3], RENEE L. BARDINI[1], GERHARD BAUER[1], KYLE D. FINK[1], BRIAN FURY[1], KYLE J. HENDRIX[1], FREDERIC CHEDIN[4], SAMIR EL-ANDALOUSSI[5,6], BILLIE HWANG[7], MICHAEL S. MULLIGAN[7], JANNE LEHTIÖ[2] AND JAN A. NOLTA[1]

1. Stem Cell Program, Department of Internal Medicine, University of California Davis; 2. Cancer Proteomics, Department of Oncology-Pathology, Karolinska Institutet; 3. Surgical and Radiological Sciences, Department of Veterinary Medicine, University of California Davis; 4. Department of Molecular and Cellular Biology, University of California Davis; 5. Department of Laboratory Medicine, Karolinska Institutet, Stockholm, Sweden; 6. Department of Physiology, Anatomy and Genetics, University of Oxford, UK; Department of Surgery, University of Washington.

Correspondence: Johnathon D. Anderson, Ph.D., Institute for Regenerative Cures, University of California Davis Medical Center, 2921 Stockton Blvd, Room 1300, Sacramento, CA 95817, Email: joanderson@ucdavis.edu, Phone: (916)-703-9300, Fax: (916)-703-9310; This work is supported by: NIH Transformative R01GM099688, NSF GRFP 2011116000, NIH T32-GM008799, NSF GROW 201111600, T32-HL086350

Received May 07, 2015; accepted for publication October 22, 2015; available online without subscription through the open access option.

1066-5099/2016/$30.00/0

This article has been accepted for publication and undergone full peer review but has not been through the copyediting, typesetting, pagination and proofreading process which may lead to differences between this version and the Version of Record. Please cite this article as doi: 10.1002/stem.2298

Key words. Mesenchymal stem cells • exosomes • proteomics • peripheral arterial disease • NFkB • HiRIEF LC-MS/MS

ABSTRACT

Mesenchymal stem cells (MSC) are known to facilitate healing of ischemic tissue related diseases through proangiogenic secretory proteins. Recent studies further show that MSC derived exosomes function as paracrine effectors of angiogenesis, however, the identity of which components of the exosome proteome responsible for this effect remains elusive. To address this we used high-resolution isoelectric focusing coupled liquid chromatography tandem mass spectrometry (HiRIEF LC-MS/MS), an unbiased high throughput proteomics approach to comprehensively characterize the proteinaceous contents of MSCs and MSC derived exosomes. We probed the proteome of MSCs and MSC derived exosomes from cells cultured under expansion conditions and under ischemic tissue simulated conditions to elucidate key angiogenic paracrine effectors present and potentially differentially expressed in these conditions. In total, 6,342 proteins were identified in MSCs and 1,927 proteins in MSC derived exosomes, representing to our knowledge the first time these proteomes have been probed comprehensively. Multi-layered analyses identified several putative paracrine effectors of angiogenesis present in MSC exosomes and increased in expression in MSCs exposed to ischemic tissue-simulated conditions; these include platelet derived growth factor (PDGF), epidermal growth factor (EGF), fibroblast growth factor (FGF) and most notably nuclear factor-kappaB (NFkB) signaling pathway proteins. NFkB signaling was identified as a key mediator of MSC exosome induced angiogenesis in endothelial cells by functional *in vitro* validation using a specific inhibitor. Collectively, the results of our proteomic analysis show that MSC derived exosomes contain a robust profile of angiogenic paracrine effectors, which have potential for the treatment of ischemic tissue-related diseases. STEM CELLS *2015; 00:000–000*

SIGNIFICANCE STATEMENT

The clinical relevance of MSC-based therapeutics has been firmly established ahead of the field's understanding of how their beneficial effects are medi-

ated. Interestingly, MSC-derived exosomes are gaining momentum in the field as a putative surrogate to MSC-based therapeutics with a stronger safety profile. Indeed the first patient has already been successfully treated with MSC-exosomes for GvHD. Our study is the first to comprehensively characterize the functional protein contents of MSC and their exosomes thereby shedding light on how they mediate their beneficial effects in the clinic and may lead to more efficacious precision-engineered MSC-based therapeutics

INTRODUCTION

Ischemic tissue related diseases such as peripheral arterial disease (PAD) affect 8-12 million people every year in the US and often there are no satisfactory treatment options for many of these patients. PAD is characterized by a lack of proper blood flow to the lower extremities due to narrowing or blockage of arterial vasculature from atherosclerotic plaques [1]. Angioplasty and stent placement are commonly used to treat PAD, however, restenosis and re-occlusion from subsequent blood clot formation and stent overgrowth limit the effectiveness of these treatments in many patients [2, 3]. A potential alternative therapeutic approach is localized induction of angiogenesis to restore blood flow to affected tissues. Several studies in animal models of PAD have shown localized induction of angiogenesis via recombinant VEGF therapy to be beneficial. However, this straightforward approach has so far failed to show clear benefits in humans in late-stage clinical trials, perhaps due to the use of a monotherapeutic approach which only targeted a single signaling pathway responsible for only one portion of the tissue healing process in PAD [4].

Bone marrow derived mesenchymal stem cells (MSCs) exhibit tissue healing capabilities via signaling to endogenous cell populations including immune cells and endothelial cells [5]. MSCs have also shown promise as a potential therapeutic for PAD through the secretion of a robust profile of angiogenic signaling proteins, however, it remains unclear which factors are the main drivers of MSC induced angiogenesis [6]. Exosomes are small lipid-bound, cellularly secreted vesicles that mediate intercellular communication via cell-to-cell transport of proteins and RNA [7]. Interestingly, exosomes have been recently shown to also mediate some of the tissue healing properties of MSCs [8-10], however, the underlying mechanisms by which MSC derived exosomes exert their tissue healing properties remain unclear.

Additionally, the angiogenic potential of MSCs can vary due to differences in their microenvironment [11]. MSCs are generally expanded in high serum (10-20%) containing media under atmospheric oxygen (normoxic) conditions (21% O_2) prior to injection into animal models [12]. However, MSCs experience a markedly different environmental niche upon injection into tissues affected by PAD, where they are exposed to significantly reduced oxygen tension and a reduced concentration of factors contained in serum due to a lack of proper blood flow [13]. It has been recognized that the angiogenic potential of endothelial cells is enhanced when stimulated under hypoxic conditions [14]. Although there is evidence that hypoxic stimulation induces expression of angiogenic signaling proteins in endothelial cells, it is not clear to what extent such changes in the environmental niche affect the MSC proteome [15, 16]. Therefore, we characterized signaling pathways and gene networks that are differentially expressed at the protein level in MSCs exposed to PAD-like culture conditions as compared to normoxic, high serum expansion conditions.

As proteins mediate most intracellular activity and communication between cells, mass spectrometry proteomics approaches have been invaluable in elucidating differential cell states and patterns of cellular communication [17]. However, mass spectrometry based proteomics approaches have had limitations in depth of analysis, greatly limiting the characterization of signaling proteins within cells as they are often present at low levels as compared to other classes of proteins such as structural proteins, which are present at much higher levels [18]. Recently we developed a new mass spectrometry approach termed high-resolution isoelectric focusing liquid coupled chromatography tandem mass spectrometry (HiRIEF LC-MS/MS), that enable deep proteome coverage of cellular lysates [19]. This approach has been demonstrated by Branca *et al* to be capable of quantitatively characterizing >10,000 proteins per cell lysate, whereas other methods of mass spectrometry generate datasets with smaller depth of coverage [19].

Here we focus on investigating the effects of a PAD-like microenvironment on angiogenic signaling protein expression within MSCs and their secreted exosomes. We use HiRIEF LC-MS/MS to investigate changes in MSC proteomic expression when cultured under normoxic, high serum expansion conditions as compared to conditions that mimic the microenvironment experienced by MSCs upon injection into tissues affected by PAD. We find that exposure of MSCs to a PAD-like microenvironment increases expression of several pro-angiogenic signaling associated proteins including epithelial growth factor (EGF), fibroblast growth factor (FGF) and platelet derived growth factor (PDGF). In addition, we find that exposure of MSCs to a PAD-like microenvironment induces elevated exosome secretion and that these secreted exosomes contain a robust angiogenic signaling profile and are capable of inducing angiogenesis *in vitro* via the nuclear factor kappa-light-chain enhancer of activated B-cells (NFkB) pathway.

MATERIAL AND METHODS

Cell culture and reagents

Human bone marrow aspirates from young adult, non-smoking males were obtain from Lonza (Allendale, NJ, www.lonza.com). For MSC isolation and expansion, bone marrow aspirates were passed through 90 μm pore strainers for isolation of bone spicules. Then, the strained bone marrow aspirates were diluted with equal volume of phosphate-buffered saline (PBS) and centrifuged over Ficoll (GE Healthcare, Waukesha, WI, www.ge-healthcare.com) for 30 minutes at 700*g*. Next, mononuclear cells and bone spicules were plated in plastic culture flasks, using minimum essential media α (MEM-α) (HyClone Thermo Scientific, Waltham, MA, www.hyclone.com) supplemented with 10% fetal bovine serum (FBS; Atlanta Biologicals, Lawrenceville, GA, www.atlantabio.com) that had been screened for optimal MSC growth. After 2 days, nonadherent cells were removed by 2–3 washing steps with PBS. After passage 2 MSCs were expanded in 20% FBS and MSCs from passages 5-6 were used for experimentation. For serum starvation studies MSCs were washed 3 times with PBS and cultured in exosome isolation media consisting of OptiMEM without phenol red with 1% L-Glut (IC) (Life Technologies, Carlsbad, CA http://www.lifetechnologies.com) for 40 hours. For serum starvation plus low oxygen conditions (PAD) MSC were cultured in exosome isolation media under 1% oxygen tension for 40 hours. Pooled human HUVECS were purchased from Lonza (Allendale, NJ, www.lonza.com) and cultured according to manufacturers instructions using EndoGRO-LS Complete media from Millipore (Billerica, MA, www.emdmillipore.com).

Vesicle isolation and characterization

MSC were washed 3 times with PBS and switched to exosome isolation media; either 20% FBS media that was pre-cleared of exosomes via 18 hour 120,000 x g centrifugation, or OptiMEM (Life Technologies, Carlsbad, CA www.lifetechnologies.com) and were conditioned for 40 hours prior to vesicle isolation [9]. Microvesicles (MV) were isolated as in previous studies [20]. Briefly conditioned media was cleared of cells and cell debris via centrifugation (500 x g and 1000 x g respectively), then spun at 17,000 x g pellet to isolate MVs. Exosomes were isolated as in previous studies [20]. Briefly, for proteomics studies exosomes were isolated using 0.22 µm filtration to get rid of cells, cell debris and microvesicles prior to being spun at 120,000 x g for 2 hours, the pellet was then washed with 39 mLs of PBS and spun again at 120,000 x g for 2 hours. All ultracentrifuge steps were performed with a Ti70 rotor in polyallomer quick seal tubes (Beckman Coulter, Brea, CA www.beckmancoulter.com). Vesicle concentration was determined using DC assay (BioRad, Hercules, CA www.bio-rad.com) and size distribution assessed using NanoSight LM10HS (Malvern, Amesbury, MA www.malvern.com).

Electron microscopy

SEM images were taken with Philips XL30 TMP, (FEI Company, Hillsboro, OR www.fei.com). Sputter Coater: Pelco Auto Sputter Coater SC-7, (Ted Pella Inc., Redding, CA www.tepella.com). TEM images were taken on Philips CM120 Biotwin Lens, 9 (FEI Company, Hillsboro, OR www.fei.com), with 2% uranyl acetate staining using facilities at Electron Microscopy Laboratory, School of Medicine, University of California at Davis.

Sample preparation for proteomics

Cell pellets were lysed with 4% SDS, 25 mM HEPES, 1mM DTT. EVs were lysed with 2% SDS, 25 mM HEPES, 1mM DTT. Lysates were heated to 95°C for 5 min followed by sonication for 1 min and centrifugation, 14.000g for 15 min. The supernatant was mixed with 1mM DTT, 8 M urea, 25 mM HEPES, pH 7.6 and transferred to a centrifugation filtering unit, 10 kDa cutoff (Nanosep®, Pall, Port Washington, NY www.pall.com), and centrifuged for 15 min, 14.000g, followed by another addition of the 8 M urea buffer and centrifugation. Proteins were alkylated by 50 mM IAA, in 8 M urea, 25 mM HEPES for 10 min, centrifuged for 15 min, 14.000g, followed by 2 more additions and centrifugations with 8 M urea, 25 mM HEPES. Trypsin (Promega, Madison WI www.promega.com), 1:50, trypsin:protein, was added to the cell lysate in 250 mM urea, 50 mM HEPES and incubated overnight at 37°C. The filter units were centrifuged for 15 min, 14,000g, followed by another centrifugation with MQ and the flow-through was collected [19]. Peptides from EVs were TMT6 labelled and MSC cells with TMT10 labelled according to manufacturer's instructions (Thermo Fisher Scientific, San Jose, CA www.thermofisher.com). Peptides were cleaned by a strata-X-C-cartridge (Phenomenex, Torrance, CA www.phenomenex.com [19, 21]).

Proteomics on nLC-MS/MS on Thermo Scientific LTQ Orbitrap Velos

Before analysis of exosomes on LTQ-Orbitrap Velos (Thermo Fischer Scientific, San Jose, CA www.thermofisher.com), peptides were separated using an Agilent 1200 nano-LC system. Samples were trapped on a Zorbax 300SB-C18, and separated on a NTCC-360/100-5-153 (Nikkyo Technos., Ltd, Tokyo, Japan www.nikkyo-tec.co.jp) column using a gradient of A (5% DMSO, 0.1% FA) and B (90% ACN, 5% DMSO, 0.1% FA), ranging from 3 % to 40% B in 45 min with a flow of 0.4 µl/min. The LTQ-Orbitrap Velos was operated in a data-dependent manner, selecting 5 precursors for sequential fragmentation by CID and HCD, and analyzed by the linear iontrap and orbitrap, respectively. The survey scan was performed in the Orbitrap at 30.000 resolution (profile mode) from 300-2000 m/z with a max injection time of 500 ms and AGC set to 1 x 10^6

ions. For generation of HCD fragmentation spectra, a max ion injection time of 500 ms and AGC of 5 x 10^4 were used before fragmentation at 37.5% normalized collision energy. For FTMS MS2 spectra, normal mass range was used, centroiding the data at 7500 resolution. Peptides for CID were accumulated for a max ion injection time of 200 ms and AGC of 3 x 10^4, fragmented with 35% collision energy, wideband activation on, activation q 0.25, activation time 10 ms before analysis at normal scan rate and mass range in the linear iontrap. Precursors were isolated with a width of 2 m/z and put on the exclusion list for 60 s. Single and unassigned charge states were rejected from precursor selection.

Proteomic data analysis

GraphPAD Prism was used to calculate differential expression using multiple t-tests and a stringent false discovery cut off of 1% (GraphPAD Prism, La Jolla, CA www.graphpad.com). Panther Pathway analysis was used to detect the number of pathways detected in each sample and the number of proteins of each pathway represented in each sample (www.pantherdb.com). Ingenuity Pathway Analysis software was used to analyze enrichment for signaling pathway proteins and putative functionality of proteins present in and between each sample (Qiagen, Redwood City, CA www.ingenuity.com). ClueGO software was used for gene ontology analysis of each sample to detected broad classes of protein functionality (www.ici.upmc.fr/cluego/cluegoDownload.shtml). CytoScape was used to generate network interactome maps for the angiogenesis interactome of MSCs and exosomes and the NFkB pathway interactome (www.cytoscape.org). The constructed angiome dataset from Chu *et al* was used to search for the presence of canonical angiogenesis mediating proteins in our data, with the addition of physically interacting proteins not found in the Chu *et al* dataset. The Spike database was used to detect proteins for which there was experimental evidence for physical interactions (ie yeast-2-hybrid, co-immunoprecipitation) with the Chu *et al* dataset and was accessed via CytoScape.

Tubule formation migration assay

Primary human umbilical cord vein endothelial cells were purchased from Lonza (Allendale, NJ, www.lonza.com) and cultured in EndoGRO-LS Complete (Millipore, Billerica, MA, www.emdmillipore.com) media as per manufacturer's protocol and plated on growth factor reduced matrigel (Corning, Corning, NY www.corning.com) and stained with Calcein AM (Life Technologies, Carlsbad, CA www.lifetechnologies.com) and imaged at 16 hours post stimulation at 4X on a Kenyence BZ-9000F (Keyence, Osaka, Japan www.keyence.com). EndoGRO basal media was used for control and exosome stimulated wells and EndoGRO-LS Complete was used as a positive control (Millipore, Billerica, MA, www.emdmillipore.com). For NFkB inhibitor experiments pyrrolidine dithiocarbamate was used at a concentration of 50 μM.

RESULTS

MSCs exposed to PAD-like conditions show dynamic proteomic changes

To address what effect PAD-like microenvironment conditions have on the proteomic profile of MSCs, HiRIEF LC/MS-MS was used to quantify the proteome of MSCs. Human MSCs derived from the bone marrow of 3 young adult, non-smoking male donors were cultured under normoxic, high serum expansion conditions until passage 6. After three PBS washes, MSCs were cultured under one of three culture conditions for 40 hours: Normoxic, high serum expansion conditions (EX: 20% FBS, 21% O_2), PAD-like conditions (PAD: 0% FBS, 1% O_2) or an intermediate condition (IC: 0% FBS, 21% O_2) (Figure 1A).

A total of 6,342 proteins were identified and quantified in each of the 9 MSC samples, with 3 donors for each of the 3 conditions (Table S1). A total of 580 membrane associated proteins were detected in each of the 9 MSC samples, including canonical MSC surface markers: CD73 (NT5E), CD90 (THY1) and CD105 (ENG) (Fig S1, Table S2, S3). Our data overlaps with and expands beyond the work by Mindaye *et al*. Statistical analysis of protein expression levels using a false discovery rate of 1% (FDR1%) revealed 315 and 843 differentially expressed proteins respectively between the EX vs IC and EX vs PAD conditions (Table S4, S5). Analysis of MSC differential expression ratios versus abundance (area) revealed differentially expressed proteins were distributed across the range of abundances of all cellular proteins (Fig 1). This indicated that the effects of the culture conditions on protein expression were not limited to lowly expressed proteins. Analysis of MSC differential expression ratios versus P-value demonstrated that significantly differentially expressed proteins (FDR1%) were distributed across the range of ratios for all cellular proteins. This indicated that the effects of the culture conditions on protein expression included many new and highly significant findings (Fig 1).

Although global heatmap cluster analysis and linear regression analysis of PAD/EX ratios revealed donor to donor variation in MSCs, it also revealed robust intra-condition concordance between donors (Fig 2, S2), especially of significantly differentially expressed proteins. MSCs exposed to PAD-like conditions showed significant increases (FDR1%) in rate limiting proteins of glycolysis (ALDOB, ENO3 and PGK1) and the NRF2/glutathione pathway (ASK1, MKK3/6 and FTH1), which are metabolic and antioxidant associated pathways that have been shown to be modulated with exposure to lower oxygen tension (Fig 1, Fig S3, S4 [22, 23]). IC-conditioned MSCs, in contrast, showed no such increases (FDR1%) in glycolysis and glutathione related pathway proteins as compared to the EX condition. Gene ontology analysis

using Cytoscape's ClueGO plugin of significantly differentially expressed proteins (FDR1%), revealed numerous cell cycle checkpoint-related pathways (G1 phase, G2/M phase and cytokinesis) involved in the regulation of cellular proliferation were downregulated in both IC and PAD conditions as compared to the EX condition (Fig S5-S9). Cholesterol and lipid biosynthesis pathways were upregulated in both IC and PAD conditions as compared to the EX condition (Fig 2, S10, S11 [24]).

Exposure of MSCs to a PAD-like environment induced significant changes in their proteome. Previous studies have indicated that MSCs are capable of inducing angiogenesis, therefore, we analyzed how this PAD-like microenvironment modulated levels of their angiogenic signaling proteins [25-27]. To investigate the interaction patterns of known angiogenic proteins in MSCs and to elucidate proteins that physically interact with these known angiogenic proteins, we developed an angiogenesis interactome network map of the MSC proteome. To generate the angiogenesis interactome network map we derived a list of known angiogenic proteins from Chu *et al* that were shown to be present in the MSC proteome [28]. We then used CytoScape to include proteins that had experimental evidence of physical interaction with these MSC exosome angiogenic proteins and to show how they interacted with each other [29]. The advantage of this approach is that it not only elucidates the physical interactions of canonical angiogenesis proteins, but additionally reveals other non-canonical proteins that physically interact with the angiome, thereby shedding light on potentially novel mediators of angiogenesis. Analysis of the angiogenesis interactome of proteins present in MSCs across all 3 donors exposed to each of the 3 conditions revealed the most robust clustering of signaling protein interactions was with platelet derived growth factor receptor (PDGFR), epidermal growth factor receptor (EGFR) and NFkB nodes (Fig S12-14). This indicates that these pathways are likely drivers of MSCs' proangiogenic potential. Furthermore, using Panther Pathway analysis, we found several angiogenic pathways to be significantly (FDR1%) upregulated in MSCs exposed to PAD-like conditions, including canonical angiogenic associated pathways of PDGF, EGF and FGF (Fig 2 [30]). These data collectively demonstrate significantly increased expression of several angiogenic signaling pathways and cholesterol/lipid biosynthesis pathways in MSCs exposed to the PAD condition as compared to the conventional EX condition.

MSC exosome secretion increases under PAD-like conditions

Newly synthesized membranes components such as lipids and cholesterol are transported from their site of genesis at the endoplasmic reticulum to the plasma membrane via vesicular transport [31, 32]. However, as cells experience decreased rates of proliferation their need for newly synthesized plasma membrane components should also decrease [33]. We observed that a variety of cell cycle pathways decreased in expression in the IC and PAD conditions as expected, since the cells were exposed to a lower oxygen tension and deprived of growth factor stimulation. Interestingly however, we observed that cholesterol/lipid biosynthesis proteins actually significantly (FDR1%) increased in expression and not decreased, in both IC and PAD conditions as compared to the expansion condition, EX (Fig S10, S11). This led us to speculate that perhaps an increase in exosome biogenesis could account for the increased expression of proteins involved in cholesterol/lipid biosynthesis. Indeed we observed a trend towards increased expression of proteins involved in the biogenesis of exosomes, prompting us to analyze vesicle secretion of MSCs (Fig S15).

Extracellular vesicles secreted from MSCs (microvesicles, exosomes) were isolated from media that had been conditioned for 40 hours under EX, IC and PAD culture conditions using ultracentrifugation. Analysis of vesicle yield via BCA protein concentration assays revealed that MSC microvesicle secretion decreased whereas exosome secretion substantially increased with MSCs exposed to IC and PAD conditions as compared to EX conditions (Fig 3). However, exosomes isolated from the EX condition co-isolated with FBS protein from the media (**Fig S16**). Scanning electron microscopy (SEM) images of MSCs exposed to PAD conditions showed vesicle structures consistent with a decrease in microvesicle secretion and an increase of exosome secretion as compared to MSC exposed to EX conditions (Fig 3). Furthermore, transmission electron microscopy of isolated PAD-derived MSC exosomes with negative staining is consistent with canonical exosome morphology; additionally, Nanosight analysis revealed that MSC exosomes were of expected size range and MSCs maintained low levels of apoptosis in all conditions (Fig 3, S16).

MSC exosome proteome contains a robust profile of angiogenic signaling proteins

As two recent studies demonstrated that MSC exosomes are pro-angiogenic both *in vitro* and *in vivo* we used MSC HiRIEF LC-MS/MS to characterize the proteome of MSC derived exosomes from MSCs exposed to IC and PAD conditions [8, 34]. A total of 1927 proteins were quantified in each of the 6 samples generated from cells derived from 3 donors under both the PAD and IC conditions (Table S1), 457 of which were not detected in MSCs, indicating exosomal enrichment (Table S6). We detected 92 of the top 100 most identified exosomal marker proteins from the ExoCarta database in each of our exosome samples from both conditions, IC and PAD (Table S7, Fig S16 [35-37]). Differential expression analysis of exosomes from IC and PAD conditions revealed few significant expression differences (FDR1%) in exosomes between IC and PAD conditions (Table S8).

Gene ontology analysis using Cytoscape's ClueGO plugin of the MSC exosome proteome from all 3 donors from both conditions showed representation of vascu-

lar and endothelial associated proteins (Fig 4 [38]). GO analyses are generally broad based and helpful for a broad overview of the data, but are generally limited in their ability to identify specific signaling pathways. We therefore performed Panther pathway analysis on the MSC exosome proteome and found high representation of several canonical angiogenic associated pathways: cadherin, EGFR, FGF and PDGF (Fig 4).

Ingenuity Pathway Analysis (IPA) is a robust high throughput data analysis software that is able to predict the induction or inhibition of various cellular activities based on an expert, manually curated database of known protein associations and functions. IPA analysis showed that MSC exosomes contain numerous proteins with a variety of angiogenesis-related functionalities including induction of: angiogenesis, vasculogenesis, cell migration and endothelial cell proliferation (Fig S17-20).

Next we performed network analysis of the angiogenesis interactome of MSC exosomes, as with the MSC proteome. We showed the most robust representation of protein nodes clustered around the canonical angiogenic pathways of NFKB1/2, Avian Reticuloendotheliosis Viral Oncogene Homolog A **(**RELA), PDGFRB and EGFR in our angiogenesis interactome network map (Fig 5). Furthermore, network analysis of the NFkB pathway showed robust representation of MSC exosome proteins clustering around RELA, NFKB1/2 and TNF-receptor associated factor 6 (TRAF6) (Fig S21). These data collectively showed that exosomes derived from MSCs exposed to PAD-like conditions contain a robust profile of angiogenic signaling proteins and putative functionalities closely mirroring those found in MSCs.

MSC exosomes induce angiogenesis via the NFkB pathway in endothelial cells

To test the angiogenic potential of MSC exosomes, human umbilical vein endothelial cells (HUVEC) were stimulated *in vitro* with PAD-derived MSC exosomes. To evaluate their ability to induce tubule formation, a canonical *in vitro* assay of angiogenesis, was applied. Traditionally, putative therapeutics are known to have a therapeutic index where they behave in a dose dependent manner with decreased effectiveness generally observed at higher doses [39]. HUVECs were treated with increasing doses of PAD-derived MSC exosomes to test for their effective dose range. The low dose of PAD-derived MSC exosomes (1 µg/mL) induced significant tubule formation compared to the unstimulated control, as did the medium dose (10 µg/mL), measured by total segment length (Fig 6). However, the high dose of PAD-derived MSC exosomes (100 µg/mL) were less effective than the medium dose indicating the upper limits of the effective dose range (Fig 6).

In our network analysis map of the MSC exosome angiogenesis interactome we observed several hubs of clustering around nodes of the NFkB complex, which is known to mediate angiogenic signaling. Even though these particular nodes, which represent core components of the NFkB complex, were not detected in the MSC exosomes we hypothesized that the presence of numerous NFkB interacting proteins may indicate a potential effector role of this pathway in HUVEC tubule formation. To test this hypothesis HUVECs were treated with pyrrolidine dithiocarbamate (PDTC), a specific inhibitor of NFkB signaling or vehicle control prior to stimulation with PAD-derived MSC exosomes in a tubule formation assay. PAD-derived MSC exosomes induced tubule formation in HUVECs treated with the vehicle control but not in HUVECs treated with PDTC, demonstrating that NFkB signaling is necessary for MSC exosome induction of tubule formation *in vitro* (Fig 7). These results indicate that MSC exosomes mediate angiogenesis in a dose dependent manner via the NFkB pathway.

DISCUSSION

This study presents, to our knowledge, the most robust proteomic characterization of MSCs and exosomes to date (MSC = 6,342 vs 1024, MSC exosome = 1927 vs 236 [40, 41]). We detected 580 membrane associated proteins including those required to meet the minimal criteria for MSC classification (CD73, CD90, CD105) across all 9 MSC samples, and represents the most robust proteomic profiling of MSC membrane proteins to date (580 vs 172 [42]). MSCs have been proposed as a therapeutic for PAD, however, the effect of the PAD microenvironment has on both the MSC physiology and MSC induced angiogenesis are poorly understood [43]. Even though several studies have demonstrated the efficacy of using MSCs for ischemic tissue related diseases, efforts towards identifying the underlying mechanisms of MSC induced angiogenesis have not been robustly investigated, as more focus has been placed on MSC secretion of VEGF and PDGF [44-47]. The quantitative proteomic methodology we used underscores the need for an unbiased approach which in the present study led to the finding that the MSC proteome is modulated upon exposure to a PAD-like microenvironment and multiple pathways are likely involved in MSC mediated angiogenesis.

We show attenuation of various cell cycle initiation and glycolysis gene networks in MSCs exposed to PAD-like conditions. Network analysis of all 3 donors from all 3 culture conditions (9 samples total) demonstrated that the MSC angiogenesis interactome is enriched for nodes associated with PDGFR, EGFR, and NFkB. This indicated that these known angiogenesis mediating pathways are likely central hubs of intracellular angiogenic signaling within MSCs [48-51]. Furthermore, when MSCs were exposed to PAD-like conditions they significantly increased expression of proteins associated with a subset of angiogenic signaling pathways EGF, FGF, and PDGF.

MSCs are known to mediate much of their tissue healing effects through their secretome in various vas-

cular disease models such as stroke and peripheral arterial disease [5, 52]. Recent studies have demonstrated that a new cell to cell communication system mediated by exosomes is capable of recapitulating much of the beneficial therapeutic effects of MSCs in these disease models [8-10, 53]. However, the underlying mechanisms by which MSC exosomes modulate these tissue healing effects have yet to be elucidated.

We characterized the proteome of exosomes derived from MSCs exposed to PAD-like conditions (PAD) and the intermediate condition (IC), but not from expansion conditions (EX) since our HiRIEF LC-MS/MS method requires large quantities of input material and the exosome yield from this condition was too small. We quantitatively characterized 1,927 proteins in MSC exosomes from all three donors across both IC and PAD conditions, of which 457 were not detected in the MSC proteome. A potential explanation for this observed protein enrichment in MSC exosomes is that some proteins can be masked in more complex lysates when using mass spectrometry methodologies, but this does not preclude the possibility that some of these proteins are being directly shuttled into exosomes for secretion [18]. Of note is the fact that the proteome of exosomes derived from MSCs appears to lack many canonical secretory signaling proteins such as cytokines and growth factors, but instead contain the downstream mediators of these pathways.

We showed that exosomes from MSCs exposed to PAD-like conditions contain a robust profile of angiogenesis associated proteins that closely mirror the upregulated angiogenic pathways found in MSCs exposed to PAD-like conditions including EGFR, FGF and PDGF pathways. These findings suggest that upon exposure to ischemic tissue conditions attempt to generate a more proangiogenic state via the secretion of exosomes, thereby facilitating localized tissue healing. An interesting unresolved question worthy of further exploration is whether the main drivers of MSC exosome induced angiogenesis act via direct signaling to endothelial cell populations or indirectly through inducing chemotaxis of immune cells such as monocytes.

We also showed that proteins mediating cholesterol/lipid biosynthesis and metabolism are significantly upregulated in MSCs that are exposed to PAD-like conditions, while several known exosome biogenesis proteins trend towards increased expression under these same conditions. Numerous cell cycle pathways are significantly downregulated in MSCs exposed to PAD-like conditions and various cell types have substantially lower rates of proliferation when exposed to similar conditions [11, 16]. Since, ostensibly there should be much less demand for such high energy cost membrane components and exosomes are known to be enriched for lipid raft components such as cholesterol [54], we therefore speculated that the upregulation of these cholesterol/lipid biosynthesis proteins may be associated with exosome secretion. We showed that MSCs increased secretion of exosomes upon exposure to PAD-like conditions which were of canonical size and morphology. Alternatively the observed increase in lipid biosynthesis may potentially be a cellular adaption to hypoxia in the PAD condition [55].

Consistent with traditional broad range small molecule dose curves, we show that exosomes derived from MSCs exposed to PAD-like conditions were able to induce angiogenesis *in vitro*, in a dose dependent manner. MSC exosomes at the highest concentration (100 µg/mL) induced less tubule formation as compared to lower doses, which may indicate an upper limit of the effective dosing range.

Our network analysis indicated that MSC exosomes derived from PAD-like conditions are enriched for several nodes associated with NFkB signaling, which has previously been shown to be an important mediator of angiogenesis [51]. We demonstrated that MSC exosome induced angiogenesis is dependent on NFkB signaling, since a specific chemical inhibitor of NFkB signaling completely abrogates the ability of MSC exosomes to induce tubule formation *in vitro*. It remains unclear, however, to what extent MSC induced angiogenesis can be attributed to exosome mediated effects. Overall, our data suggest that there are more signaling pathways involved which are worthy of further investigation.

CONCLUSION

A common trend that is becoming apparent across the MSC exosome literature is that exosomes derived from MSCs are able to mediate much of the functionality traditionally associated with canonical secretory proteins such as growth factors of the MSC secretome [8-10, 34, 56-60]. Whether canonical secretory proteins or exosomally delivered proteins are the main drivers of the MSC secretome's functionality still needs further investigation; based on our data it is likely microenvironment dependent.

An exciting open question is whether MSC exosomes derived from PAD-like culture conditions can be used as a therapeutic in lieu of MSCs for a various diseases and if so what the underlying therapeutic mechanisms might be. A study published in 2014 on the first human patient successfully treated with MSC exosomes for graft versus host disease would seem to suggest that this area of research is feasible and worthy of further investigation [9]. Our preliminary data suggest that MSC derived exosomes may be a promising therapeutic platform that provides additional benefits to the use of MSCs themselves. Our data may also provide a blueprint for future studies aiming to attempt to engineer MSC exosomes to be a more efficacious therapeutic for cardiovascular diseases.

ACKNOWLEDGMENTS

Funding provided by NIH Transformative R01GM099688, NSF GROW 201111600, NIH T32-GM008799, NIH T32 HL086350 and NSF GRFP

2011116000, SELA is supported by the Swedish Research Council (VR-Med and EuroNanoMedII).

CONFLICT OF INTEREST

None.

AUTHOR CONTRIBUTIONS

J.D.A.: Conception and design, financial support, collection and/or assembly of data, data analysis and interpretation, manuscript writing, final approval of manuscript; H.J.J.: Collection and/or assembly of data, data analysis and interpretation, manuscript writing, final approval of manuscript; C.S.G.: manuscript writing, final approval of manuscript; M.V.: Collection and/or assembly of data; M.T.P.: Collection and/or assembly of data, final approval of manuscript; C.S.B.: Collection and/or assembly of data, final approval of manuscript; E.N.M.: Collection and/or assembly of data, final approval of manuscript; M.S.M.: Collection and/or assembly of data, data analysis and interpretation, manuscript writing, final approval of manuscript; R.L.B.: Collection and/or assembly of data, data analysis and interpretation, final approval of manuscript; G.B.: Conception and design, manuscript writing, final approval of manuscript; K.D.F.: Manuscript writing, final approval of manuscript; B.F.: Conception and design, manuscript writing, final approval of manuscript; F.C.: Conception and design, manuscript writing, final approval of manuscript; S.E.A.: Conception and design, manuscript writing, final approval of manuscript J.L.: Financial support, manuscript writing, final approval of manuscript; J.A.N.: Financial support, manuscript writing, final approval of manuscript.

REFERENCES

1 Milani RV, Lavie CJ. The role of exercise training in peripheral arterial disease. *Vascular medicine* 2007; **12(**4**):** 351-358. doi: 10.1177/1358863X07083177

2 Katz G, Harchandani B, Shah B. Drug-eluting stents: the past, present, and future. *Current atherosclerosis reports* 2015; **17**(3)**:** 485. doi: 10.1007/s11883-014-0485-2

3 Banfi A, von Degenfeld G, Gianni-Barrera R, Reginato S, Merchant MJ, McDonald DM *et al.* Therapeutic angiogenesis due to balanced single-vector delivery of VEGF and PDGF-BB. *FASEB journal : official publication of the Federation of American Societies for Experimental Biology* 2012; **26**(6)**:** 2486-2497. doi: 10.1096/fj.11-197400

4 Yla-Herttuala S, Rissanen TT, Vajanto I, Hartikainen J. Vascular endothelial growth factors: biology and current status of clinical applications in cardiovascular medicine. *Journal of the American College of Cardiology* 2007; **49**(10)**:** 1015-1026. doi: 10.1016/j.jacc.2006.09.053

5 Meyerrose T, Olson S, Pontow S, Kalomoiris S, Jung Y, Annett G *et al.* Mesenchymal stem cells for the sustained in vivo delivery of bioactive factors. *Advanced drug delivery reviews* 2010; **62**(12)**:** 1167-1174. doi: 10.1016/j.addr.2010.09.013

6 Liew A, O'Brien T. Therapeutic potential for mesenchymal stem cell transplantation in critical limb ischemia. *Stem cell research & therapy* 2012; **3**(4)**:** 28. doi: 10.1186/scrt119

7 S ELA, Mager I, Breakefield XO, Wood MJ. Extracellular vesicles: biology and emerging therapeutic opportunities. *Nature reviews. Drug discovery* 2013; **12**(5)**:** 347-357. doi: 10.1038/nrd3978

8 Bian S, Zhang L, Duan L, Wang X, Min Y, Yu H. Extracellular vesicles derived from human bone marrow mesenchymal stem cells promote angiogenesis in a rat myocardial infarction model. *Journal of molecular medicine* 2014; **92**(4)**:** 387-397. doi: 10.1007/s00109-013-1110-5

9 Kordelas L, Rebmann V, Ludwig AK, Radtke S, Ruesing J, Doeppner TR *et al.* MSC-derived exosomes: a novel tool to treat therapy-refractory graft-versus-host disease. *Leukemia* 2014; **28**(4)**:** 970-973. doi: 10.1038/leu.2014.41

10 Zhang B, Wang M, Gong A, Zhang X, Wu X, Zhu Y *et al.* HucMSC-exosome mediated -Wnt4 signaling is required for cutaneous wound healing. *Stem cells* 2014. doi: 10.1002/stem.1771

11 Rosova I, Dao M, Capoccia B, Link D, Nolta JA. Hypoxic preconditioning results in increased motility and improved therapeutic potential of human mesenchymal stem cells. *Stem cells* 2008; **26**(8)**:** 2173-2182. doi: 10.1634/stemcells.2007-1104

12 Ikebe C, Suzuki K. Mesenchymal stem cells for regenerative therapy: optimization of cell preparation protocols. *BioMed research international* 2014; **2014:** 951512. doi: 10.1155/2014/951512

13 Banfi A, von Degenfeld G, Blau HM. Critical role of microenvironmental factors in angiogenesis. *Current atherosclerosis reports* 2005; **7**(3)**:** 227-234.

14 Humar R, Kiefer FN, Berns H, Resink TJ, Battegay EJ. Hypoxia enhances vascular cell proliferation and angiogenesis in vitro via rapamycin (mTOR)-dependent signaling. *FASEB journal : official publication of the Federation of American Societies for Experimental Biology* 2002; **16**(8)**:** 771-780. doi: 10.1096/fj.01-0658com

15 Yamakawa M, Liu LX, Date T, Belanger AJ, Vincent KA, Akita GY *et al.* Hypoxia-inducible factor-1 mediates activation of cultured vascular endothelial cells by inducing multiple angiogenic factors. *Circulation research* 2003; **93**(7)**:** 664-673. doi: 10.1161/01.RES.0000093984.48643.D7

16 Beegle J, Lakatos K, Kalomoiris S, Stewart H, Isseroff RR, Nolta JA *et al.* Hypoxic Preconditioning of Mesenchymal Stromal Cells Induces Metabolic Changes, Enhances Survival and Promotes Cell Retention in Vivo. *Stem cells* 2015. doi: 10.1002/stem.1976

17 Johansson HJ, Sanchez BC, Mundt F, Forshed J, Kovacs A, Panizza E *et al.* Retinoic acid receptor alpha is associated with tamoxifen resistance in breast cancer. *Nature communications* 2013; **4:** 2175. doi: 10.1038/ncomms3175

18 Hultin-Rosenberg L, Forshed J, Branca RM, Lehtio J, Johansson HJ. Defining, comparing, and improving iTRAQ quantification in mass spectrometry proteomics data. *Molecular & cellular proteomics : MCP* 2013; **12**(7)**:** 2021-2031. doi: 10.1074/mcp.M112.021592

19 Branca RM, Orre LM, Johansson HJ, Granholm V, Huss M, Perez-Bercoff A *et al.* HiRIEF LC-MS enables deep proteome coverage and unbiased proteogenomics. *Nature methods* 2014; **11**(1)**:** 59-62. doi: 10.1038/nmeth.2732

20 Witwer KW, Buzas EI, Bemis LT, Bora A, Lasser C, Lotvall J *et al.* Standardization of sample collection, isolation and analysis methods in extracellular vesicle research. *Journal of extracellular vesicles* 2013; **2**. doi: 10.3402/jev.v2i0.20360

21 Wisniewski JR, Zougman A, Nagaraj N, Mann M. Universal sample preparation method for proteome analysis. *Nature methods* 2009; **6**(5)**:** 359-362. doi: 10.1038/nmeth.1322

22 Lai JC, Behar KL. Glycolysis-citric acid cycle interrelation: a new approach and some insights in cellular and subcellular compartmentation. *Dev Neurosci* 1993; **15**(3-5)**:** 181-193.

23 Hayes JD, Dinkova-Kostova AT. The Nrf2 regulatory network provides an interface between redox and intermediary metabolism. *Trends Biochem Sci* 2014; **39**(4)**:** 199-218. doi: 10.1016/j.tibs.2014.02.002

24 Saito R, Smoot ME, Ono K, Ruscheinski J, Wang PL, Lotia S *et al.* A travel guide to Cytoscape plugins. *Nature methods* 2012; **9**(11)**:** 1069-1076. doi: 10.1038/nmeth.2212

25 Duffy GP, Ahsan T, O'Brien T, Barry F, Nerem RM. Bone marrow-derived mesenchymal stem cells promote angiogenic processes in a time- and dose-dependent manner

in vitro. *Tissue Eng Part A* 2009; **15**(9)**:** 2459-2470. doi: 10.1089/ten.TEA.2008.0341

2**6** Iwase H, Wiegel B, Fehrenbacher G, Schardt D, Nakamura T, Niita K *et al.* Comparison between calculation and measured data on secondary neutron energy spectra by heavy ion reactions from different thick targets. *Radiat Prot Dosimetry* 2005; **116**(1-4 Pt 2)**:** 640-646.

2**7** Kwon HM, Hur SM, Park KY, Kim CK, Kim YM, Kim HS *et al.* Multiple paracrine factors secreted by mesenchymal stem cells contribute to angiogenesis. *Vascular pharmacology* 2014; **63**(1)**:** 19-28. doi: 10.1016/j.vph.2014.06.004

2**8** Chu LH, Rivera CG, Popel AS, Bader JS. Constructing the angiome: a global angiogenesis protein interaction network. *Physiol Genomics* 2012; **44**(19)**:** 915-924. doi: 10.1152/physiolgenomics.00181.2011

2**9** Cline MS, Smoot M, Cerami E, Kuchinsky A, Landys N, Workman C *et al.* Integration of biological networks and gene expression data using Cytoscape. *Nat Protoc* 2007; **2**(10)**:** 2366-2382. doi: 10.1038/nprot.2007.324

3**0** Mi H, Muruganujan A, Casagrande JT, Thomas PD. Large-scale gene function analysis with the PANTHER classification system. *Nat Protoc* 2013; **8**(8)**:** 1551-1566. doi: 10.1038/nprot.2013.092

3**1** Soccio RE, Breslow JL. Intracellular cholesterol transport. *Arterioscler Thromb Vasc Biol* 2004; **24**(7)**:** 1150-1160. doi: 10.1161/01.ATV.0000131264.66417.d5

3**2** Lev S. Nonvesicular lipid transfer from the endoplasmic reticulum. *Cold Spring Harb Perspect Biol* 2012; **4**(10). doi: 10.1101/cshperspect.a013300

3**3** Baenke F, Peck B, Miess H, Schulze A. Hooked on fat: the role of lipid synthesis in cancer metabolism and tumour development. *Dis Model Mech* 2013; **6**(6)**:** 1353-1363. doi: 10.1242/dmm.011338

3**4** Zhang HC, Liu XB, Huang S, Bi XY, Wang HX, Xie LX *et al.* Microvesicles derived from human umbilical cord mesenchymal stem cells stimulated by hypoxia promote angiogenesis both in vitro and in vivo. *Stem cells and development* 2012; **21**(18)**:** 3289-3297. doi: 10.1089/scd.2012.0095

3**5** Simpson RJ, Kalra H, Mathivanan S. ExoCarta as a resource for exosomal research. *Journal of extracellular vesicles* 2012; **1**. doi: 10.3402/jev.v1i0.18374

3**6** Mathivanan S, Fahner CJ, Reid GE, Simpson RJ. ExoCarta 2012: database of exosomal proteins, RNA and lipids. *Nucleic acids research* 2012; **40**(Database issue)**:** D1241-1244. doi: 10.1093/nar/gkr828

3**7** Mathivanan S, Simpson RJ. ExoCarta: A compendium of exosomal proteins and RNA. *Proteomics* 2009; **9**(21)**:** 4997-5000. doi: 10.1002/pmic.200900351

3**8** Bindea G, Mlecnik B, Hackl H, Charoentong P, Tosolini M, Kirilovsky A *et al.* ClueGO: a Cytoscape plug-in to decipher functionally grouped gene ontology and pathway annotation networks. *Bioinformatics* 2009; **25**(8)**:** 1091-1093. doi: 10.1093/bioinformatics/btp101

3**9** Jiang W, Makhlouf F, Schuirmann DJ, Zhang X, Zheng N, Conner D *et al.* A Bioequivalence Approach for Generic Narrow Therapeutic Index Drugs: Evaluation of the Reference-Scaled Approach and Variability Comparison Criterion. *AAPS J* 2015. doi: 10.1208/s12248-015-9753-5

4**0** Kim HS, Choi DY, Yun SJ, Choi SM, Kang JW, Jung JW *et al.* Proteomic analysis of microvesicles derived from human mesenchymal stem cells. *Journal of proteome research* 2012; **11**(2)**:** 839-849. doi: 10.1021/pr200682z

4**1** Mindaye ST, Ra M, Lo Surdo JL, Bauer SR, Alterman MA. Global proteomic signature of undifferentiated human bone marrow stromal cells: evidence for donor-to-donor proteome heterogeneity. *Stem cell research* 2013; **11**(2)**:** 793-805. doi: 10.1016/j.scr.2013.05.006

4**2** Mindaye ST, Ra M, Lo Surdo J, Bauer SR, Alterman MA. Improved proteomic profiling of the cell surface of culture-expanded human bone marrow multipotent stromal cells. *Journal of proteomics* 2013; **78:** 1-14. doi: 10.1016/j.jprot.2012.10.028

4**3** Capoccia BJ, Robson DL, Levac KD, Maxwell DJ, Hohm SA, Neelamkavil MJ *et al.* Revascularization of ischemic limbs after transplantation of human bone marrow cells with high aldehyde dehydrogenase activity. *Blood* 2009; **113**(21)**:** 5340-5351. doi: 10.1182/blood-2008-04-154567

4**4** Beckermann BM, Kallifatidis G, Groth A, Frommhold D, Apel A, Mattern J *et al.* VEGF expression by mesenchymal stem cells contributes to angiogenesis in pancreatic carcinoma. *British journal of cancer* 2008; **99**(4)**:** 622-631. doi: 10.1038/sj.bjc.6604508

4**5** Deuse T, Peter C, Fedak PW, Doyle T, Reichenspurner H, Zimmermann WH *et al.* Hepatocyte growth factor or vascular endothelial growth factor gene transfer maximizes mesenchymal stem cell-based myocardial salvage after acute myocardial infarction. *Circulation* 2009; **120**(11 Suppl)**:** S247-254. doi: 10.1161/CIRCULATIONAHA.108.843680

4**6** Fierro FA, Kalomoiris S, Sondergaard CS, Nolta JA. Effects on proliferation and differentiation of multipotent bone marrow stromal cells engineered to express growth factors for combined cell and gene therapy. *Stem cells* 2011; **29**(11)**:** 1727-1737. doi: 10.1002/stem.720

4**7** Ding W, Knox TR, Tschumper RC, Wu W, Schwager SM, Boysen JC *et al.* Platelet-derived growth factor (PDGF)-PDGF receptor interaction activates bone marrow-derived mesenchymal stromal cells derived from chronic lymphocytic leukemia: implications for an angiogenic switch. *Blood* 2010; **116**(16)**:** 2984-2993. doi: 10.1182/blood-2010-02-269894

4**8** Gianni-Barrera R, Bartolomeo M, Vollmar B, Djonov V, Banfi A. Split for the cure: VEGF, PDGF-BB and intussusception in therapeutic angiogenesis. *Biochemical Society transactions* 2014; **42**(6)**:** 1637-1642. doi: 10.1042/BST20140234

4**9** Tabernero J. The role of VEGF and EGFR inhibition: implications for combining anti-VEGF and anti-EGFR agents. *Mol Cancer Res* 2007; **5**(3)**:** 203-220. doi: 10.1158/1541-7786.MCR-06-0404

5**0** Fujioka S, Sclabas GM, Schmidt C, Frederick WA, Dong QG, Abbruzzese JL *et al.* Function of nuclear factor kappaB in pancreatic cancer metastasis. *Clin Cancer Res* 2003; **9**(1)**:** 346-354.

5**1** Hou Y, Li F, Karin M, Ostrowski MC. Analysis of the IKKbeta/NF-kappaB signaling pathway during embryonic angiogenesis. *Dev Dyn* 2008; **237**(10)**:** 2926-2935. doi: 10.1002/dvdy.21723

5**2** Bronckaers A, Hilkens P, Martens W, Gervois P, Ratajczak J, Struys T *et al.* Mesenchymal stem/stromal cells as a pharmacological and therapeutic approach to accelerate angiogenesis. *Pharmacology & therapeutics* 2014; **143**(2)**:** 181-196. doi: 10.1016/j.pharmthera.2014.02.013

5**3** Lai RC, Arslan F, Lee MM, Sze NS, Choo A, Chen TS *et al.* Exosome secreted by MSC reduces myocardial ischemia/reperfusion injury. *Stem cell research* 2010; **4**(3)**:** 214-222. doi: 10.1016/j.scr.2009.12.003

5**4** Tan SS, Yin Y, Lee T, Lai RC, Yeo RW, Zhang B *et al.* Therapeutic MSC exosomes are derived from lipid raft microdomains in the plasma membrane. *Journal of extracellular vesicles* 2013; **2**. doi: 10.3402/jev.v2i0.22614

5**5** Masson N, Ratcliffe PJ. Hypoxia signaling pathways in cancer metabolism: the importance of co-selecting interconnected physiological pathways. *Cancer Metab* 2014; **2**(1)**:** 3. doi: 10.1186/2049-3002-2-3

5**6** Li T, Yan Y, Wang B, Qian H, Zhang X, Shen L *et al.* Exosomes derived from human umbilical cord mesenchymal stem cells alleviate liver fibrosis. *Stem cells and development* 2013; **22**(6)**:** 845-854. doi: 10.1089/scd.2012.0395

5**7** Katsuda T, Tsuchiya R, Kosaka N, Yoshioka Y, Takagaki K, Oki K *et al.* Human adipose tissue-derived mesenchymal stem cells secrete functional neprilysin-bound exosomes. *Scientific reports* 2013; **3:** 1197. doi: 10.1038/srep01197

5**8** Lin SS, Zhu B, Guo ZK, Huang GZ, Wang Z, Chen J *et al.* Bone marrow mesenchymal stem cell-derived microvesicles protect rat pheochromocytoma PC12 cells from glutamate-induced injury via a PI3K/Akt dependent pathway. *Neurochem Res* 2014; **39**(5)**:** 922-931. doi: 10.1007/s11064-014-1288-0

5**9** Bruno S, Grange C, Deregibus MC, Calogero RA, Saviozzi S, Collino F *et al.* Mesenchymal stem cell-derived microvesicles protect against acute tubular injury. *Journal of the American Society of Nephrology : JASN* 2009; **20**(5)**:** 1053-1067. doi: 10.1681/ASN.2008070798

6**0** Xin H, Li Y, Liu Z, Wang X, Shang X, Cui Y *et al.* MiR-133b promotes neural plasticity and functional recovery after treatment of stroke with multipotent mesenchymal stromal cells in rats via transfer of exosome-enriched extracellular particles. *Stem cells* 2013; **31**(12)**:** 2737-2746. doi: 10.1002/stem.1409


See www.StemCells.com for supporting information available online. STEM CELLS *; 00:000–000*

Figure 1. Experimental design workflow and ratio distribution of MSC proteomics. (A) Schematic representation of proteomics workflow. MSCs were isolated from human bone marrow and expanded to passage 6 using expansion (EX) conditions. Cells were then washed 3 times with PBS and switched to either expansion (EX), intermediate (IC) or PAD-like (PAD) conditions for 40 hours. Cells or exosomes were then lysed, trypsinized and ran on high-resolution isoelectric focusing (HiRIEF) strips which were divided into 72 individual fractions and ran on liquid chromatography tandem mass spectrometry (LC-MS/MS). Identified proteins were analyzed using 3 different types of analysis software: gene ontology, canonical signaling pathways and network analysis of the angiome interactome. ClueGO gene ontology analysis was used to characterize enrichment for proteins based on their functionalities. Panther and IPA pathway analysis was used to characterize enrichment for proteins of specific canonical signaling pathways. CytoScape network analysis of the angiome interactome was used to visualize the physical interactions of known angiogenesis-mediating proteins (angiome) with proteins for which there is experimental evidence of physical interaction. **(B)** Plot of PAD/EX ratios (Log2, fold change) versus area (Log10, abundance) of MSC proteins; red dots represent significantly differentially expressed proteins (FDR1%), blue dots represent all non- significantly differentially expressed proteins. **(C)** PAD/EX ratios (Log2, fold change) versus P-value; yellow dots represent differentially expressed proteins with mean fold changes < +/- 0.5 Log2, red dots represent > +/- 0.5 Log2 mean fold change with p-value < 0.01 and blue dots with a p-value of > 0.01.

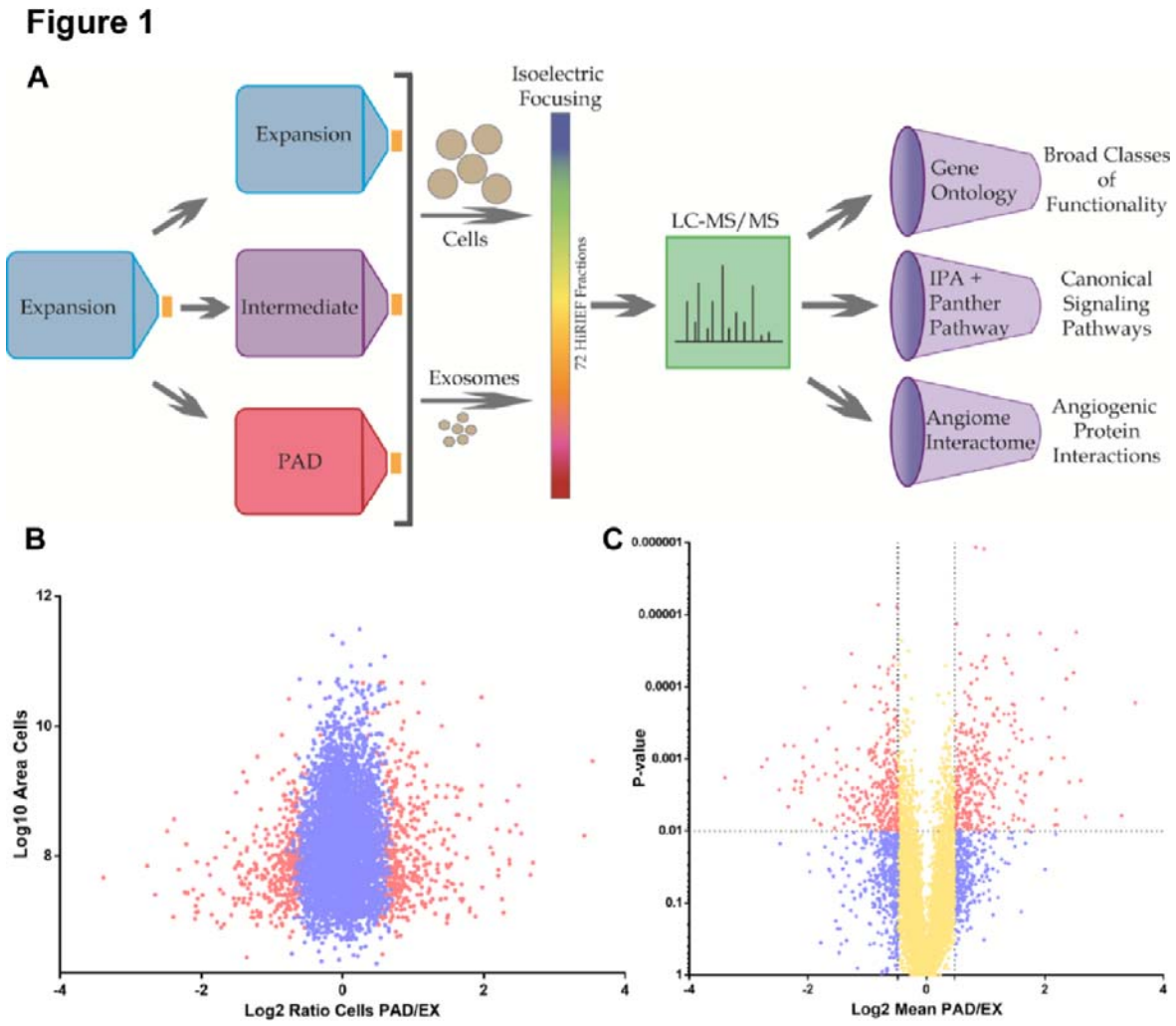

Figure 2. Analysis of HiRIEF LC-MS/MS proteomics data from IC and PAD conditions compared to control condition EX. **(A)** Heatmap of MSC cluster analysis of differentially regulated proteins in IC and PAD conditions as compared to EX. **(B)** ClueGO gene ontology analysis of proteins upregulated in PAD MSCs shows enrichment for cholesterol biosynthesis, lipid biosynthesis, angiogenesis and glycolysis associated proteins. **(C)** Panther pathway analysis of proteins upregulated in MSCs under PAD-like conditions show abundance of canonical angiogenesis related pathway proteins: EGF, FGF and PDGF (red asterisk indicate angiogenesis associated pathways). Analysis of 3 different donors for each condition. For differential expression T-tests with multiple testing correction with an FDR of 1% was used. Circles are color coded according to their associated functionality. Number of circles and larger diameter of circles indicate greater over representation.

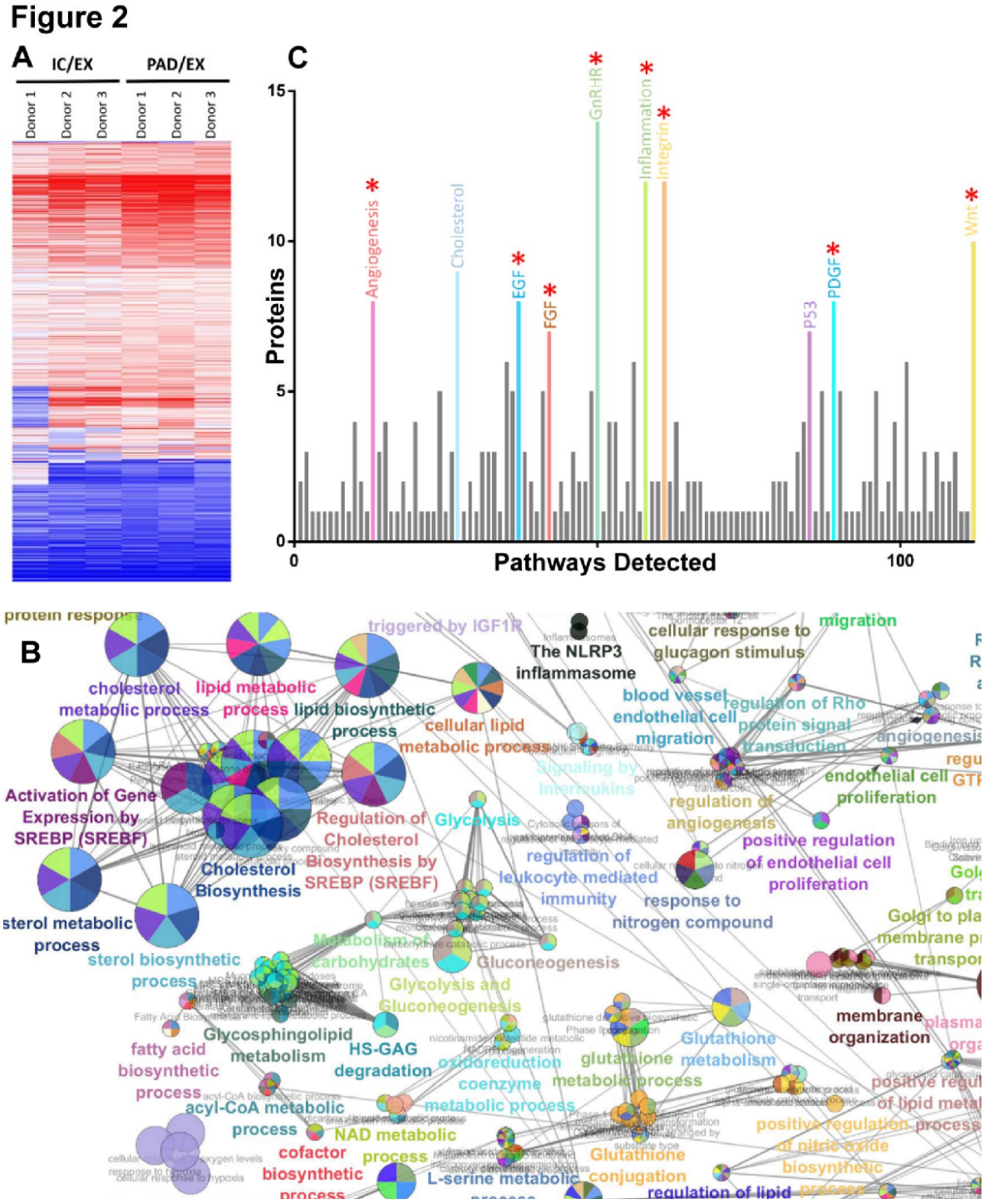

Figure 3. Mesenchymal stem cells increase secretion of exosomes upon exposure to PAD-like conditions. **(A)** Quantification of total protein content of vesicles derived from MSC under EX, IC and PAD culture conditions using DC assay. **(B)** Scanning electron micrograph of MSCs cultured in EX culture conditions indicating microvesicle release (blue arrows) from the cell surface (scale bar 5 um, 5kX). **(C)** Scanning electron micrograph of MSCs cultured under PAD conditions (scale bar 2 um, 10kX) indicating exosome adhesion to cell surface (red arrows). **(D)** Transmission electron micrograph of MSC derived exosomes with 2% uranyl acetate negative staining (scale bar 200 nm, 25kX).

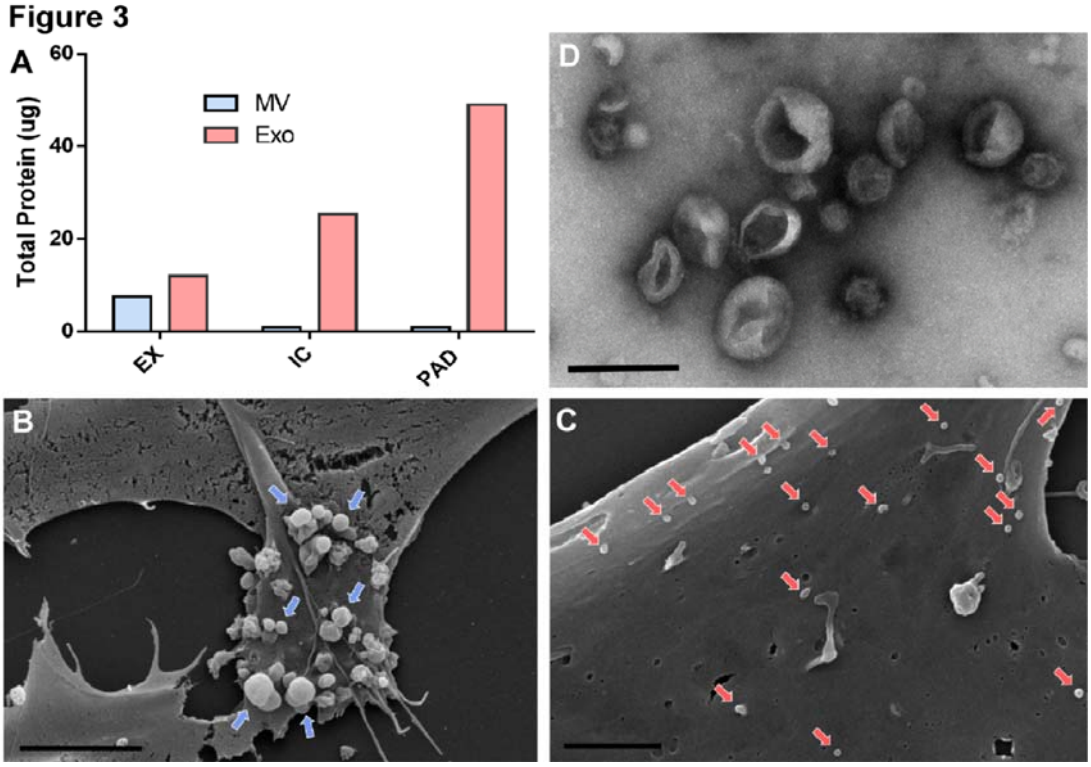

Figure 4. Analysis of HiRIEF LC-MS/MS proteomics data of MSC exosomes comparing PAD to IC conditions. **(A)** ClueGO network analysis of 400 most abundant proteins in PAD exosomes shows enrichment for effector proteins (blue boxes). **(B)** Panther pathway analysis of PAD exosomes shows abundance of angiogenesis related pathway proteins: EGFR, FGF and PDGF pathway associated proteins (red asterisk indicate angiogenesis associated pathways). Analysis of 3 different donors for each condition. For differential expression T-tests with multiple testing correction with an FDR of 1% was used. Circles are color coded according to their associated functionality. Number of circles and larger diameter of circles indicate greater over representation.

Figure 4

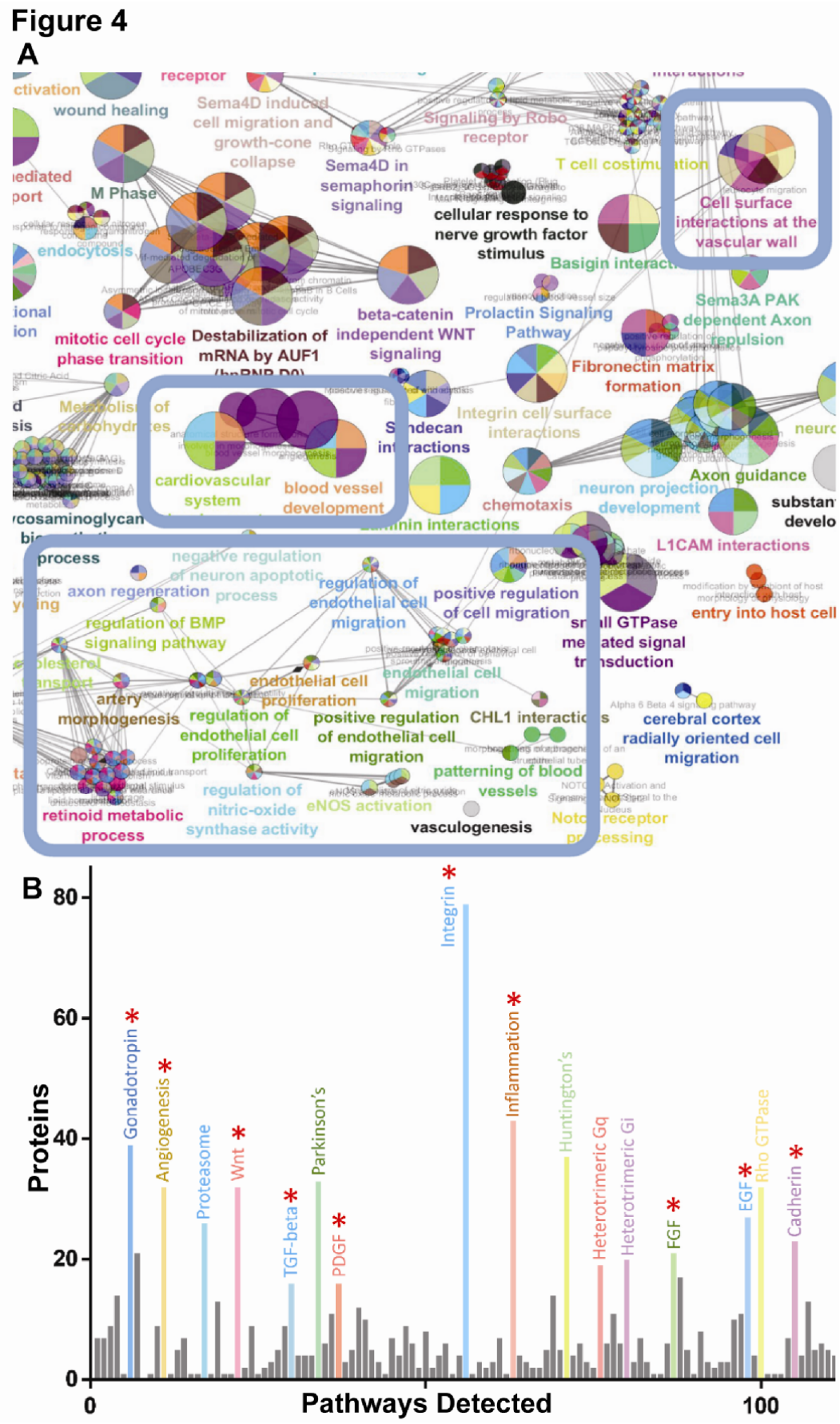

Figure 5. Network analysis of MSC exosome angiogenesis interactome. Network analysis using CytoScape of the MSC exosome angiogenesis interactome reveals clustering around nodes involved in NFkB signaling (emboldened boxes). Red boxes indicates presence in angiome interacting proteins in MSC exosomes, blue boxes indicate absence of these network proteins in MSC exosomes. Boxes of major clustering nodes of known effectors were enlarged for clarity. Edges connecting boxes indicates experimental evidence of physical contact (eg co-immunopreciptitation, yeast-2-hybrid).

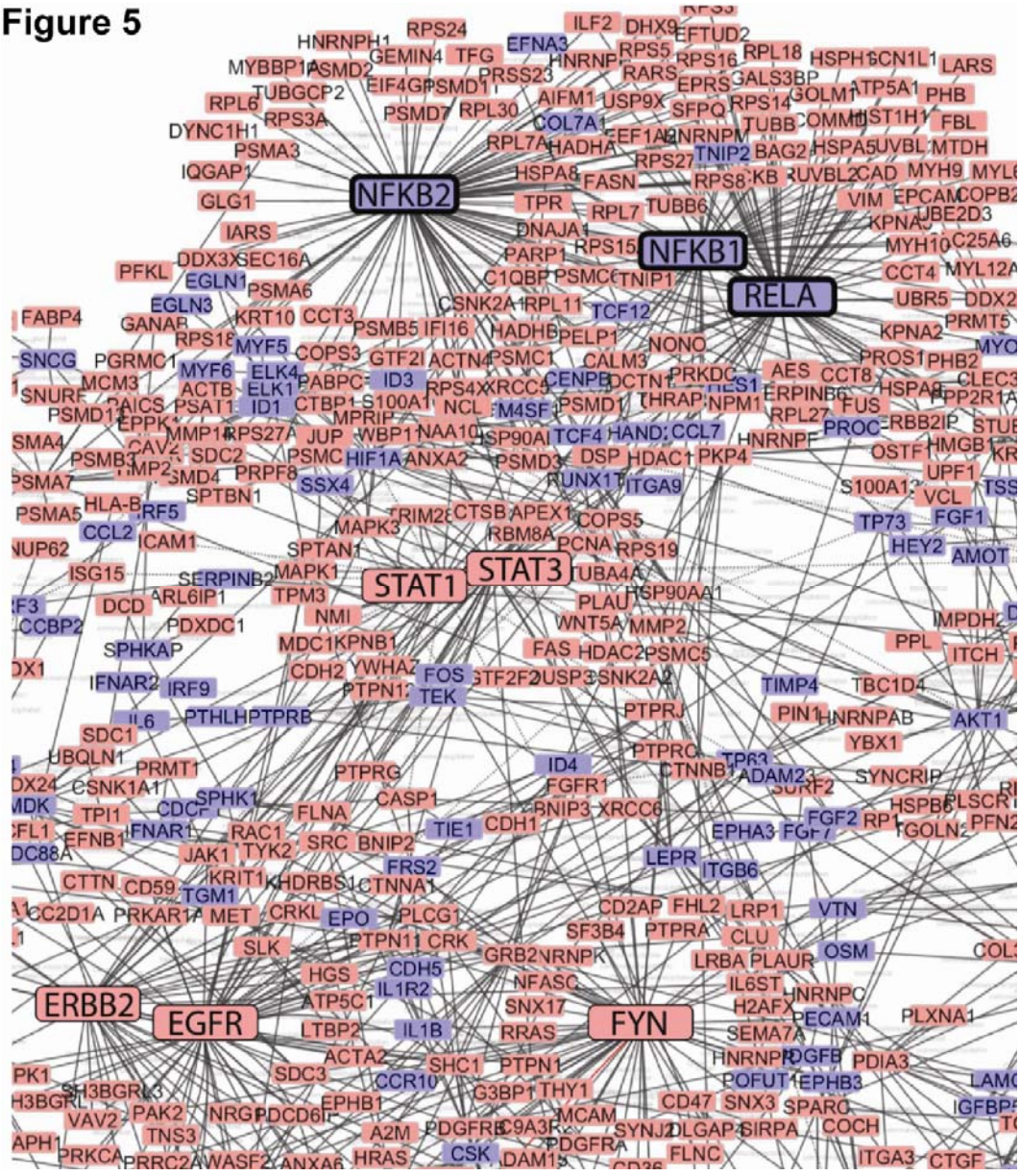

Figure 6. MSC exosome-induced *in vitro* tubule formation of HUVECs. **(A)** Basal media (Neg), **(B)** 5 ug/ml, **(C)** 10 ug/ml, **(D)** 20 ug/ml of MSC exosomes in basal media, **(E)** EndoGRO media positive control (Pos). Stained with Calcein AM and imaged at 14 hours post stimulation with 4X objective. **(F)** Quantification of total segment length of tubule formation analyzed using ImageJ's Angiogenesis plugin. EndoGRO positive control media contains 2% FBS, EGF 5ng/ml and heparin sulfate 0.75 U/ml. (*) Indicates a p-value <0.05 using ANOVA, LSD post hoc analysis (n = 12).

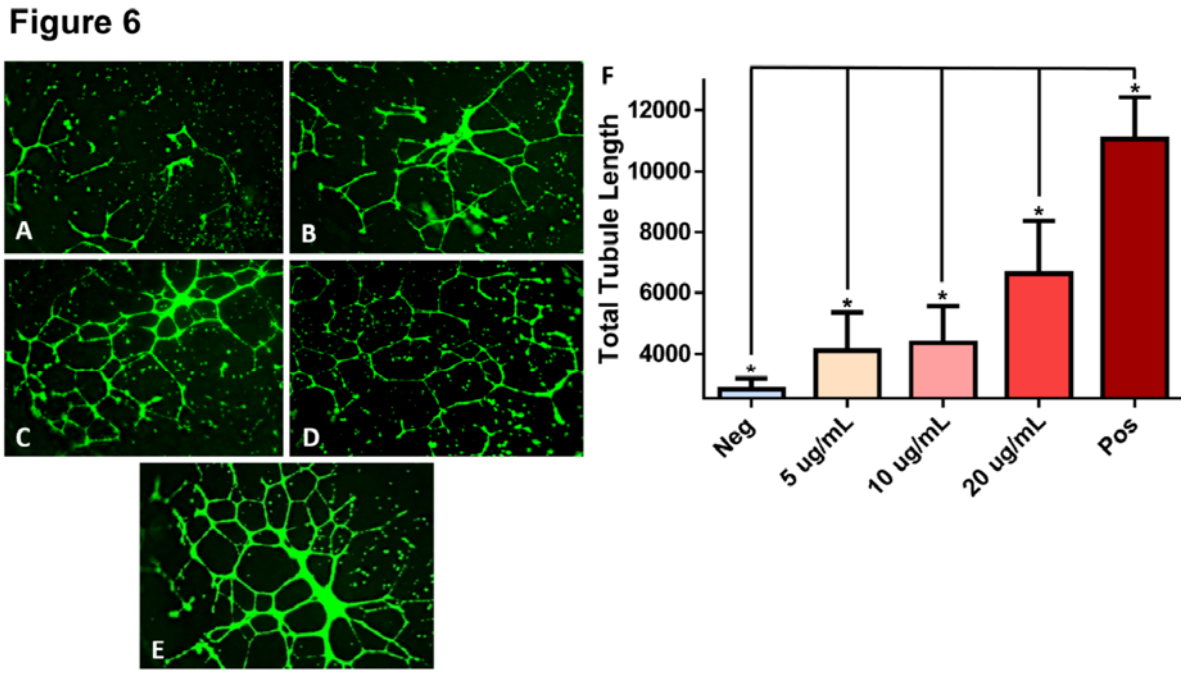

Figure 7. NFkB inhibition abrogates MSC exosome-mediated tubule formation in HUVECs *in vitro*. (A) basal media, **(B)** basal media + NFkB inhibitor, **(C)** 10 ug/ml, **(D)** 10 ug/ml + NFkB inhibitor, **(E)** EndoGRO media, **(F)** EndoGRO media + NFkB inhibitor. HUVECs stained with Calcein AM and imaged 14 hours post stimulation with a 4X objective. **(G)** Quantification of total segment length of tubule formation using ImageJ's Angiogenesis plugin. EndoGRO media contains 2% FBS, EGF 5ng/ml and heparin sulfate 0.75 U/ml. (*) Indicates a p-value <0.01 using ANOVA, LSD post hoc analysis (n = 6).

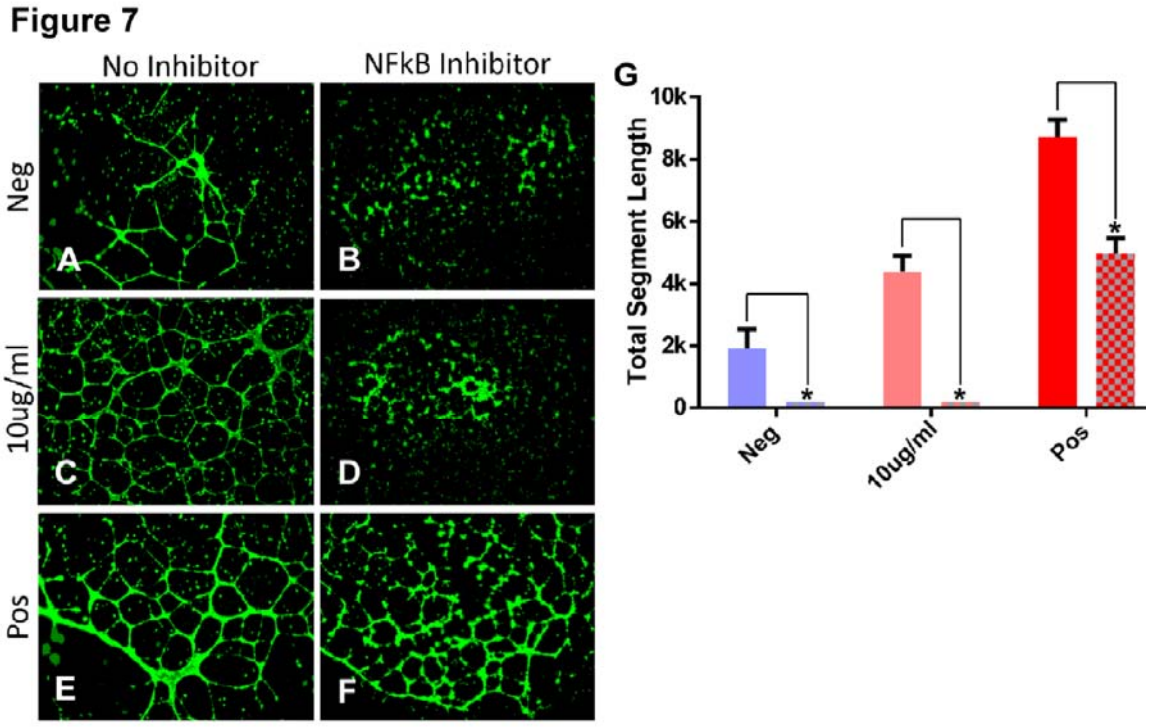

Graphical Abstract

Mesenchymal stem cells (MSCs) exposed to peripheral arterial disease-like (PAD) conditions increase expression of a diverse profile of angiogenic proteins which are subsequently packaged into exosome for secretion and induce angiogenesis in endothelial cells.